IGF-1 Gene Therapy Modifies Inflammatory Environment and Gene Expression in the Caudate-Putamen of Aged Female Rat Brain

Eugenia Falomir-Lockhart
CCT La Plata: CONICET La Plata
Franco Juan Cruz Dolcetti
CCT La Plata: CONICET La Plata
Macarena Lorena Herrera
CONICET Cordoba
Jerónimo Pennini
CCT La Plata: CONICET La Plata
María Florencia Zappa Villar
CCT La Plata: CONICET La Plata
Gabriela Salinas
Universitatsmedizin Gottingen
Enrique Portiansky
UNLP: Universidad Nacional de la Plata
Björn Spittau
Bielefeld University: Universitat Bielefeld
Ezequiel Lacunza
UNLP: Universidad Nacional de la Plata
Claudia Beatriz Hereñú
CONICET Cordoba
Maria Jose Bellini (mariajosebellini@yahoo.com)
National University of La Plata https://orcid.org/0000-0001-5737-9101

Research Article

Keywords: IGF-1 gene therapy, neuroinflammation, RNA-seq, aged brain, microglia

Posted Date: June 29th, 2021

DOI: https://doi.org/10.21203/rs.3.rs-638414/v1

Abstract

Brain aging is characterized by chronic neuroinflammation caused by activation of glial cells, mainly microglia, leading to alterations in homeostasis of the central nervous system. Microglial cells are constantly surveying their environment to detect and respond to diverse signals. During aging, microglia undergo a process of senescence, characterized by loss of ramifications, spheroid formation, and fragmented processes, among other abnormalities. Therefore, the study of microglia senescence is of great relevance to understand age-related declines in cognitive and motor function.

We have targeted the deleterious effects of aging by implementing gene therapy with IGF-1, employing recombinant adenoviral vectors (RAds) as a delivery system. In this study, we performed intracerebroventricular (ICV) IGF-1 gene therapy on aged female rats and evaluated its effect on Caudate-Putamen unit (CPu) gene expression and inflammatory state. IGF-1 gene therapy modified senescent microglia of the CPu towards an anti-inflammatory state increasing the proportion of $Iba1^{+}Arg1^{+}$ cells. Moreover, IGF-1 gene therapy was able to regulate the pro-inflammatory environment of CPu in female aged rats by down-regulating the expression of genes typically over-expressed during aging. Our results demonstrate that, ICV IGF-1 gene therapy, is capable to modulate microglia cells and CPu gene expression, leading to an improvement in motor function.

Introduction

Brain aging is characterized by chronic neuroinflammation caused by activation of glial cells, mainly microglia, in response to the accumulation of oxidative damage, mitochondrial dysfunction and loss of proteostasis that lead to alterations in homeostasis of the central nervous system (CNS) (López-Otín et al., 2013). Neuroinflammation has been implicated in the aetiology and progression of many neurodegenerative diseases, such as Alzheimer's disease and Parkinson's disease (Bassani et al., 2015; Di Benedetto et al., 2017). Under these pathological conditions, glial cells undergo genotypic and morphological changes, and increase the secretion of inflammatory mediators such as cytokines and free radicals, as well as neurotrophins, growth factors, and extracellular matrix proteins (Orihuela et al., 2016). In summary, these cells can either promote survival or induce death of nearby neurons, glial cells themselves, and other cell types.

Microglia cells are constantly surveying their environment. By doing so, these cells are able to detect diverse extracellular signals and, consequently, elaborate a response in order to maintain brain homeostasis (Elward and Gasque, 2003). Nevertheless, during normal aging, microglial cells undergo a senescence process characterized by loss of ramifications, spheroid formation, gnarling, and fragmented processes, among others (Harry GJ, 2013). These alterations are different from the morphological changes occurring during microglial activation. Senescent microglia present a dystrophic morphology that can be observed, almost exclusively, in elder subjects. We believe that the study of microglia senescence is of great relevance to understand age-related declines in neural functions.

Insulin-like growth factor-1 (IGF-1) is a powerful neurotrophic and neuroprotective factor of great interest for neuronal rescue in neurodegenerative processes (Acaz-Fonseca et al., 2015; Labandeira-Garcia et al., 2017; Suh et al., 2013). It has been broadly described that IGF-1 exerts neuroprotective actions in the CNS under different conditions *in vitro* (Bellini et al., 2011) and *in vivo* (Morel et al., 2017; Piriz et al., 2011; Torres Aleman, 2012), including the aged brain (Deak and Sonntag, 2012; Falomir-Lockhart et al., 2019; Herrera et al., 2020; Labandeira-Garcia et al., 2017; Piriz et al., 2011). In response to different insults, the brain increases the production of growth factors, including IGF-1. Furthermore, this factor has been used successfully as a therapeutic agent in different experimental models of neurodegeneration and neuronal damage (Breese et al., 1996; Genis et al., 2014).

Considering the role that microglia play in the brain functional decline during aging, we decided to investigate whether IGF-1 could modulate brain environment in aged animals.

We have previously reported the use of recombinant adenovirus carrying the IGF-1 transgene (RAd-IGF1) to increase IGF-1 expression in the brain parenchyma (Hereñú et al., 2009, 2007). Moreover, our group has demonstrated that the intracerebroventricular (ICV) administration of RAd-IGF1 restored the rate of neurogenesis in the hippocampus and corrected the cognitive (Pardo et al., 2016) and motor (Nishida et al., 2011) deficits in aged rats.

Aging is associated with nigrostriatal system alterations leading to motor dysfunction. Although the decrease in the number of nigral cells due to age remains controversial (Alladi et al., 2009; Parkinson et al., 2015; Stark and Pakkenberg, 2004), it has been described that there is a decrease in the levels of Dopamine (DA), the main neurotransmitter involved in the regulation of motor function (Carlsson and Winblad, 1976), and its receptors, particularly the Dopamine Receptor 2 (D2R) (Morgan and Finch, 1988; Umegaki et al., 2008) in CPu. Roth et al. demonstrated that increasing the density of dopamine receptors through pharmacological intervention improves motor function in senile rats (JOSEPH and ROTH, 1988).

Here, we aimed to study the effects of ICV gene therapy with RAd-IGF-1 on CPu gene expression, microglia inflammatory state and dopamine transporter and receptors in the aging brain. Considering the anti-inflammatory potential of IGF-1, we postulate that this intervention constitutes an effective strategy to modulate the inflammatory environment that contributes to microglia senescence.

Materials And Methods

2.1. Animals

Female aged Sprague-Dawley rats (28-months-old) weighing 270 ± 25 g) were used. This rat strain has a maximum life expectancy of 36 months (Johns Hopkins University, Animal Care and Use Committee). Animals were housed in a temperature-controlled room (22 ± 2 ºC) on a 12:12 h light/dark cycle and fed *ad libitum*, with a standard chow diet containing 12.08 kJ/g calories: 69.5 % carbohydrates, 5.6 % fat, and 24.9 % protein (Asociacion de Cooperativas Argentinas-S.E.N.A.S.A. No. 04-288/A). All experiments with animals were performed according to the Animal Welfare Guidelines of NIH (INIBIOLP's Animal Welfare Assurance No A5647-01). The ethical acceptability of the animal protocols used here has been approved by our institutional Committee for the Care and Use of Laboratory Animals (Protocol #T09-01-2013).

2.2. Adenoviral Vectors

We employed recombinant adenoviral vectors (RAd) previously constructed in our laboratory (Hereñú et al., 2007) as carriers to deliver either the therapeutic cDNA of IGF-1 gene (RAd-IGF-1) or the red fluorescent protein from Discosoma sp. DsRed (RAd-DsRed).

2.3. Experimental design

Experimental day 0 (D0) was defined as the day of the stereotaxic injections. From day − 3 (D-3) to D-1, animals were assessed on behavioural tests (more details below). On D0, rats were anesthetized with ketamine hydrochloride (40 mg/kg; i.p.) plus xylazine (8 mg/kg; i.m.) and placed in a stereotaxic apparatus. Rats were randomly divided into two groups (n = 21–24 per group): DsRed group, which received an injection of RAd-DsRed; and IGF-1 group, which received an injection of RAd-IGF-1. Bilateral injections in the lateral ventricles were performed placing the tip of a 26 G needle fitted to a 10 µL syringe at the following coordinates relative to the Bregma: − 0.8 mm anteroposterior, − 4.2 mm dorsoventral and ± 1.5 mm mediolateral (Paxinos and Watson, 2007). Rats were injected with 8 µL per side of a suspension containing $4x10^{10}$ plaque forming units (pfu) of the appropriate vector. On D15 to D17, animals were re-assessed on behavioural tests. Finally, on experimental D18, animals were euthanized by rapid decapitation and their brains were removed. Left hemispheres were stored in 4 % paraformaldehyde, pH 7.4, overnight at 4°C and then kept in

cryoprotectant solution (30 % de ethylene glycol, 30 % de sucrose, in PB 0.1 M, pH 7.4) at − 20°C until use for immunostaining assays. Right hemispheres were dissected and stored at -80°C for later RNA or protein extraction (see below). Body weight was determined every 2 or 3 days from D-5 before surgery until the end of the experiment.

2.4. Behavioural Tests

2.4.1. Open Field. Open Field (OF) test was carried out to evaluate locomotion function before (D-3) and after (D16) treatment. Animals were placed on an open arena (65 cm x 65 cm x 45 cm) for 5 min. Animals' behaviour was recorded with a digital camera (Logitech). Then, the total distance travelled by each animal, expressed in meters, was measured using Kinovea software v0.7.6 (http://www.kinovea.org).

2.4.2. Performance on a wire mesh ramp. Wire Mesh Ramp test was carried out to evaluate motor function before (D-1) and after (D17) treatment (Nishida et al., 2011). A 90 cm long by 42 cm wide metal ramp set at an angle of 70° to the floor was used and submerged into water up to 15 cm to prevent the animals from descending to the floor. Animals were placed on the central strip and the latency for them to fall to the water was recorded as the average of two consecutive tests. The maximum time for the animal to stay at the platform was 120 sec.

2.4.3. Performance on a rotating platform. Rotating Platform test was carried out to evaluate motor function before (D-1) and after (D17) treatment (Nishida et al., 2011). Animals were placed on the centre of an elevated cylindrical plastic platform (30 cm height, 8 cm diameter) and the motor was immediately turned on at 30 rpm. The latency for the animals to fall off the platform was recorded as the average of two consecutive tests.

2.4.4. Marble Burying. Marble Burying (MB) test is based on the observation that rodents bury either harmful or harmless objects (e.g., glass marbles) in their bedding (Poling et al., 1981). This behavioural test has been considered a species-typical behaviour and has been related to hoarding in rats (de Brouwer et al., 2019; Poling et al., 1981; Thomas et al., 2009). MB test was carried out on D15 after ICV-RAds injection. Individual subjects were placed in a housing cage (30 × 30 × 17 cm) with 5 cm of fresh hardwood chip bedding. An array of 16 glass marbles (1.5 cm in diameter, arranged in a 4 × 4 grid) was evenly spaced over the surface. The number of marbles intact, moved, sunken and/or buried during a 30-min period was analysed. In this procedure, a marble was considered "moved" if it was changed from its original position, "sunken" if 2/3 of it was covered with bedding, and "buried" if at least 3/3 of the marble was covered with bedding and at a distance of 3 cm or less from the bottom (Deacon, 2006).

2.5. Immunostaining

All immunohistochemical techniques were performed on free-floating sections of 40 µm under moderate shaking. Washes and incubations were done in 0.1 M phosphate buffer, pH 7.4, containing 0.3% triton X-100 and 5% NSG (washing buffer). From each rat, one in every twelve serial sections was selected to obtain a set of non-contiguous serial sections spanning the CPu or the Substantia Nigra. For double staining with Arginase-1 and Iba1, sections were incubated during 48 h at 4°C with the following primary antibodies: polyclonal rabbit anti-Iba1 diluted 1:1000 (WAKO CTG2683) and polyclonal goat anti-Arginase1 diluted 1:200 (Santa Cruz, N-20 sc-18351). After three washes in buffer, sections were incubated for 2 h with donkey anti-Rabbit-Alexa 488 conjugated antibody, diluted 1:1000 (Jackson ImmunoResearch, Code 711-545-144) together with donkey anti-goat-Cy3 conjugated IgG, diluted 1:1000 (Jackson ImmunoResearch, Code 705-165-003). For tyrosine hydroxylase (TH)-neurons detection, sections were incubated for 48 h at 4°C with polyclonal rabbit anti-TH antibody, diluted 1:500 (Millipore, #AB152). After three washes in buffer, sections were incubated for 2 h with goat anti-rabbit-Alexa 488 conjugated IgG, diluted 1:500 (Abcam, #AB150077). In both staining, sections were mounted on gelatinized slides. Coverslips were mounted with Fluoromount-G (eBioscience).

2.6. Image Analysis

Immunostained tissues with anti-TH antibodies were imaged using a video camera mounted on a Nikon Eclipse E400 microscope. Double stained tissues were imaged using a confocal microscope (Olympus FV1000). In both cases, the acquired images were analysed using Image J software (NIH).

Regarding microglia/macrophages immunostaining, between 25 and 70 $Iba1^+$ cells per animal were counted and analysed for their colocalization with Arginase 1. Quantification of double positive cells (Arg1 and Iba1 staining) colocalizing in the same plane was carried out using a 40x magnifying objective.

To determine density of TH-positive neurons in the Substantia Nigra, images were taken using a 40x magnifying objective. Then, the area of interest was defined in accordance with the rat brain atlas (Paxinos and Watson, 2007) and all TH-positive cell bodies were manually counted. To determine density of TH-positive fibres in the CPu, images were taken using a 60x magnifying objective. The density of fibres was determine using the grid technique as described by von Bohlen and Halbach (2013) (Von Bohlen Und Halbach, 2013). In our analysis, a grid of 200 μm^2 per frame was employed. Six or 8 frames per animal were analysed. Relative fibre density was expressed as Q = Gi/Go, where Gi is the grid points intercepted by the fibres and Go is the total number of grid points (256 in our grid).

All quantifications were done manually by an observer blind to experimental conditions.

2.7. Western Blot

2.7.1 Sample Preparation. In order to obtain protein lysates, right CPu and Substantia Nigra were homogenized with precooled Tissue Protein Extraction Reagent (T-PER, Thermo Scientific, #78510) supplemented with Halt Protease Inhibitory Cocktail (Thermo Scientific, #78440). Finally, protein concentration was measured by Bradford protein assay using the Pierce BCA Protein Assay kit (Thermo Scientific, #23225). Bovine serum albumin (BSA, 0.1–1 mg/ml) was used as a standard. Samples were aliquoted and stored at -80°C.

2.7.2. Immunoblotting. Equal amounts of protein (20 µg) for every sample were separated by 4–20% gradient SDS-PAGE (Mini-PROTEAN TGX Precast Protein Gels, BioRad) and transferred to PVDF membranes (Bio-Rad). Membranes were blocked by incubation in 5% fetal bovine serum (FBS) in Tris-buffered saline/Tween-20 (TBS-T) for 1 h at room temperature and then incubated with primary antibodies against rabbit TH diluted 1:500 (Abcam, #AB152) or rabbit β-actin diluted 1:5000 (Cell Signalling, #8457), overnight at 4°C. Then, membranes were washed with TBS-T and incubated with the secondary anti-rabbit antibody conjugated with horseradish peroxidase diluted 1:10000 (Cell Signalling, #7074) for 2 h at room temperature. Then, membranes were washed with TBS to eliminate excess of secondary antibody. Visualization was performed with SignalFire™ Elite ECL Reagent (Cell Signalling, #12757). The signal was captured by exposure to a radiographic plate (Santa Cruz Biotechnologies) in a developing cassette for Western Blot. Relative optical density of TH bands was analysed and normalized to relative density of the β-actin band using Image Studio Lite software.

Phophorilation of Akt and Erk1/2 was analysed employing the PathScan® Intracellular Signaling Array Kit (Cell Signaling Technology, #7323) according to manufacturer’s procedure.

2.8. qRT-PCR

Total RNA was extracted from four CPu per group using TranZol reagent (Roche) according to the manufacturer's instructions. Gene expression levels were measured employing Luna® One-Step kit (New England Biolabs, #E3005) and a real time PCR CFX Connect Real-Time System (Bio-Rad) according to the manufacturer's instructions. A total of 200 ng was used to measure TH expression, while 30 ng were used to measure the housekeeping expression. The following primers were used: TH-Fw TCGGAAGCTGATTGCAGAGA; TH-Rv TTCCGCTGTGTATTCCACATG; GAPDH-Fw

TCACCACCATGGAGAAGGC; GAPDH-Rv GCTAAGCAGTTGGTGGTGCA. The $2^{(-\Delta\Delta CT)}$ method was used as the measurement method.

2.9. RNA extraction, library preparation, and sequencing

Total RNA was extracted from three samples per group using Monarch Total RNA Miniprep kit (New England Biolabs®) according to the manufacturer's instructions. The quality of the isolated RNA was assessed by measuring the RIN (RNA Integrity Number) using the Fragment Analyzer. Library preparation for RNA-Seq was performed using the truSeq RNA Sample Preparation Kit (Illumina, Cat. N° RS-122-2002) starting from 500 ng of total RNA. Accurate quantitation of cDNA libraries was performed using the QuantiFluor TM dsDNA System (Promega). The size range of final cDNA libraries was 280–320 bp and was determined applying the DNA Chip for NGS Libraries using the Fragment Analyzer (Advanced Analytical). cDNA libraries were amplified and sequenced by using the cBot and HiSeq2000 from Illumina (SR; 50 bp; ca. 30–35 million reads per sample).

2.10. RNA-Seq data analysis

Illumina HiSeq 2000 fluorescence images were transformed to BCL files with the Illumina BaseCaller software and samples were demultiplexed to FASTQ files with CASAVA (version 1.8.2). Sequencing quality was checked and approved via the FastQC software. Sequences were aligned to the genome reference sequence of Rattus norvegicus (RGSC assembly v6.0) using the HISAT2 alignment software (Kim et al., 2019). To assign to the genomic features the mapped reads that were generated from RNA sequencing, BAM files were processed with the Counts function feature from the RSubread R package (Liao et al., 2019). After the RNA sequencing of the 6 samples included in the study and prior to perform differentially expressed genes (DEG) analysis, we applied Multidimensional scaling (MDS) which is a multivariate data analysis approach used to visualize the similarity/dissimilarity between samples by plotting points (each sample) in two dimensional plots. The analysis led us to exclude one sample of each predefined group, because they behaved as outliers. Despite this, the grouping of the remaining samples and the distance between the groups was sufficiently robust to perform the analysis with duplicates **(Figure S1).**

Next, to identify DEG between *CPu* samples from IGF-1 and DsRed rats, the DESeq2 algorithm based on the normalized number of counts mapped to each gene (Love et al., 2014) was used.

Functional enrichment analysis of DEGs (p-adj. < 0.05; Fold Changes > 2) was performed with the ClueGo plugin of the Cystoscape software in order to capture the biological processes associated to IGF-1 therapy (Mlecnik et al., 2018). Overrepresented GO terms as well as KEGG/Reactome/Wikipathways pathways were functionally organized into GO/pathway term network.

For gene aging related comparisons the GenAge database (http://genomics.senescence.info/genes/) was used, from which we obtained and explored into a database of genes commonly altered during aging, built from a microarray meta-analysis study that included 27 different experiments from mice, rats and humans comprising almost 5 million gene expression measurements from over 400 individual samples (de Magalhães et al., 2009).

2.11. Statistical Analysis

Data shown in the figures are presented as the mean ± standard error of the mean (SEM). The size of the experimental groups is indicated in each figure legend. Gaussian distribution of data sets was assessed by Kolmogorov-Smirnov test. Statistical analysis was performed by using the software GraphPad Prism 8 (GraphPad Software). P-values < 0.05 were considered significant.

Results

3.1. IGF-1 gene therapy improves motor performance of aged rats

Previously, we demonstrated that ICV IGF-1 gene therapy improves grip strength during motor performance evaluation in aged rats (Nishida et al., 2011). To expand our knowledge on how IGF-1 gene therapy can influence other brain functions, locomotion and social behaviour were tested on aged rats before and after treatment with either IGF-1 expressing or DsRed-expressing adenoviral vectors.

Locomotion was assessed by measuring the travelled distance in an Open Field setting. No significant differences between groups before or after the treatment were observed (Fig. 1A-B). Moreover, after treatment with either RAd-DsRed or RAd-IGF-1, all animals decrease the travelled distance (Fig. 1C).

We also analysed the innate social behaviour to burry objects found in the cage bedding using the Marble Burying test. In order to avoid a decreased in burrowing activity by preexposure to the burying substrate (de Brouwer et al., 2019), we measured MB only at the end of the study. No significant differences in the number of intact, moved, sunken or buried marbles between groups were observed (Fig. 2).

For motor performance, we evaluated forelimbs and hindlimbs functionality using the Wire Mesh Ramp test and the Rotating Platform test. We observed that IGF-1 gene therapy improved motor performance of aged rats in both tests (Rotating Platform test: Fig. 3A, P = 0.0104; Wire mesh ramp test: Fig. 3B, P = 0.0207). These results are in accordance with previous results obtained by our group (Nishida et al., 2011).

3.2. ICV IGF-1 gene therapy does not alter the dopaminergic system

Since IGF-1 gene therapy only induced an improvement in grip strength, the question arose as to whether this pattern could be due to any structural or functional alteration in the dopaminergic (DA) system. In order to address this question, we quantified the number of DA neurons in the *Substantia nigra* and the density of DA fibres in the CPu. No significant differences between groups were observed (Fig. 4; **C** *Substantia nigra*: t-test, P = 0.6091; **D** CPu: t-test, P = 0.8247). Furthermore, we assessed the expression of tyrosine hydroxylase (TH) through Western Blot analysis in both areas and through qPCR in the CPu. Once again, no significant differences between DsRed and IGF-1 groups neither in the protein levels, nor in the mRNA levels of TH were detected (**Figure S2; C** Western blot: **Substantia nigra**: t-test, P = 0.2246; **D** CPu: t-test, P = 0.7002; qPCR **E**: t-test, P = 0.4291). Finally, the expression of DA receptors 1 and 2 (D1R and D2R), and DA transporter (DAT) through qPCR in the CPu was assessed. Again, no significant differences in the mRNA levels of these genes were observed between DsRed and IGF-1 groups. Nevertheless, the group treated with RAd-IGF-1 showed a tendency to increase the expression of D2R in the CPu (P = 0.0595) (**Figure S3; A** D1R: t-test, P = 0.6588; **B** D2R: t-test, P = 0.0595; **C** DAT: t-test, P = 0.6320).

3.3. IGF-1 gene therapy modifies microglia/macrophages phenotype in aged brains

In previous reports, it was demonstrated that ICV-IGF-1 gene therapy increases the number (DsRed Vs IGF-1: 25960 ± 2177 Vs 37666 ± 2815 cells/mm^3; P < 0.0001) and reactivity (34.64 ± 6.11 Vs 52.4 ± 4.639 %; P = 0.0008) of Iba1 positive cells, specifically in the CPu (Falomir-Lockhart et al., 2019). Nevertheless, morphological analysis of these cells gives us no information regarding their inflammatory phenotype. Moreover, changes in glia cells phenotypes might be implicated in the motor impairment observed in aged rats. Consequently, we decided to determine the proportion of anti-inflammatory M2 microglia/macrophages by measuring anti-Iba1 and anti-Arginase1 specific marker expression. Quantification of Iba1$^+$Arg1$^+$ cells revealed that RAd-IGF-1 treatment promotes microglial/macrophages polarization

towards an anti-inflammatory phenotype, showed by the increment in the number of double positive cells in the CPu (Fig. 5D).

3.4. IGF-1 gene therapy regulates aging gene expression in the CPu.

Finally, we wondered whether IGF-1 gene therapy induced any dysregulation in gene expression that would affect microglial activity in the CPu. Therefore, to understand the effect of RAd-IGF-1 therapy as compared to RAd-DsRed controls, high throughput RNA sequencing was performed. Analysis showed 97 differentially expressed genes (DEG), all down-modulated in the IGF-1 group compared to the DsRed one (LogFC > |1|, p value < 0.05; **Table S1**). Heat map representation in Fig. 6A shows the enrichment level of the top 70 genes.

Pathway analysis of DEG showed changes on several related immune processes, among others (Fig. 6B). To deepen our understanding of the relationship between these pathways, we performed functional enrichment analysis which allow the visualization of non-redundant biological terms for large clusters of genes in a functionally grouped network. Results revealed 14 main clusters ($p < 0.001$) highlighting the close association among most of them (Fig. 6C, **Table S2**). Clusters are indicated in the figure with their respective names and colours. Each cluster can be made up of one or more interconnected circles of the same colour. Each circle represents a biological term related to the broader ontological term that names the cluster **(Table S2)**. Each cluster and their biological terms are significantly ($p < 0.001$) overrepresented by a group of related DEG (**Table S2**). Among them it is worth mentioning processes such as Neuroinflammatory response (with the genes Aif1, Ptprc, Tlr7), Pro-inflammatory response (C3, Casp1, Mefv), Microglial cell activation (Aif1, Ptprc, Tlr7), Complement activation (C1r, C1s, C2, C3), TYROBP causal network (C3, Cd4, Cxcl16, Plek) and Regulation of cytokine biosynthetic process (Cd4, Cd74, Cd86, Cybb, Irf1, Ptprc, Tlr7) (**Table S2**).

Given that the DEG found in our study were mostly down-modulated after RAd-IGF1 treatment, we decided to assess this list of DEG in a physiological aging context. A search for genes commonly altered during aging in the database GenAge was carried out. A dataset drawn from a microarray meta-analysis study, consisting of 366 genes, of which 225 are commonly up-modulated in aging while 141 are down-modulated was used (**Table S2**). When this list is compared with our DEG list we found 12 genes (12-gene list) in common, all up-modulated during aging according to the meta-analysis dataset (Fig. 6D). As shown in Table 1, the over-expression or up-regulation of the 12-gene list has been associated with pathological conditions, trauma and/or neuroinflammation. These results are in accordance with our hypothesis that the anti-inflammatory effect of IGF-1 can modulate the pro-inflammatory environment caused by aging in the brain of aged rats.

Table 1
Pathways and pathologies associated to the 12-gene list

Gene Symbol	Gene Name	Cell source	CNS/Aging/Neuroinflammation	Publication	p-value
C3	Complement C3	Microglia/macrophage	Associated with neuronal and synaptic loss in the hippocampus and cognitive decline; Involved in microglial phagocytic activity	[32–35]	3,03E-05
C1s	C1s and C1r subcomponents of C1 complex	Microglia and astrocytes	Complement classical pathway activation has been associated to neuronal loss and neuroinflammation in AD. Absence of C1s and C1r subcomponents prevents the assembly of C1 complex and, thus, activation of the pathway.	[35–38]	2,35E-09
C1r					2,77E-05
GBP2	Guanylate binding protein 2	Neurons and microglia	Up-regulated in TBI. Promotes neuronal apoptosis	[39]	3,45E-10
B2M	Beta-2 microglobulin	Not specified	Major contributor to age-related cognitive decline. Pro-aging factor. Up-regulated in interferon response.	[40,41]	2,73E-06
CD74	Cluster de diferenciación 74	Microglia/macrophage and astrocytes	UP-regulated in AD in astrocytes and microglia	[42,43]	4,54E-07
CP	Ceruloplasmin	Astrocytes	Increased levels of CP are found in cerebrospinal fluid of patients with AD. It has been shown that activates microglia and increases microglial iNOS activity under pro-inflammatory stimuli.	[44,45]	2,95E-07
PSMB8	Proteasome subunit beta 8	Microglia/macrophages and astrocytes	Mutations causes autoinflammatories disorders. Association of PSMB8-AS1 is upregulated in glioma tissues and cells and promotes cell differentiation. In glioblastoma, PSMB8 inhibition induces apoptosis and blocks migration and invasion via PI3K/AKT regulation, and regulates angiogenesis by reducing VEGF expression.	[46–48]	9,45E-05
PLEK	Pleckstrin	All	Has been associated with Schizophrenia (a polymorphism and regulation of signalling pathways). Pleckstrin is a critical molecule for pro-inflammatory cytokine secretion (TNF- and IL-1B) in response to elevated AGE in diabetes. May contribute to the synaptic failure and cognitive dysfunction in AD.	[49–51]	6,48E-05

Gene Symbol	Gene Name	Cell source	CNS/Aging/Neuroinflammation	Publication	p-value
FCGR3A	Fc fragment of IgG receptor IIIa	Microglia	Up-regulated after TBI in hippocampus. Up-regulated in prefrontal cortex in Schizophrenia.	[52,53]	6,05E-05
RT1-Bb	Rano class II histocompatibility antigen, B-1 beta chain	Microglia/ Macrophages	Changes with increasing age. Changes in aging in hippocampus, PFC and behavioural correlation. Transcriptomic profile in female aged rats.	[54,55]	1,47E-06
CXCL16	C-X-C motif chemokine ligand 16	Microglia/ Macrophages	Up-regulated in aging. Involved in AD, cognitive decline, modulating neurotransmitter release in hippocampal CA1 area.	[41,56]	7,72E-05

It is worth noting that no genes related to IGF-1R pathway were found to be differentially expressed. We believe that this could be due to the time window between RAd injection and animal sacrifice. Nevertheless, we evaluated the activation of Akt and Erk1/2 proteins, both involved in IGF-1 response downstream IGF-1 receptor. We observed that phosphorylation of Akt at Ser473 was increased in CPu of animals treated with RAd-IGF-1 (t-test, P = 0.0118), while no significant differences were observed in Akt phosphorylation at Thr308 (t-test, P = 0.3967) or Erk1/2 (t-test, P = 0.4888) (Fig. 7).

Discussion

Our research group has set the goal to combat the deleterious effects of aging in aged rats by implementing gene therapy with IGF-1, employing recombinant adenoviral vectors (RAds) as a delivery system. This growth factor has demonstrated to be neuroprotective in different experimental models. Thus, the injection of IGF-1 in a cerebellar deference ataxia model is able to promote re-innervation, recovering the total motor activity (Fernandez et al., 1998). Additionally, IGF-1 plays a neuroprotective role in hypoxia-ischemia models, where it is able to reduce the loss of cholinergic and GABAergic neurons (Guan et al., 1999). Moreover, IGF-1 gene therapy abrogates the excitotoxic damage induced by kainic acid in the spinal cord (Nishida et al., 2020). Furthermore, our group has demonstrated that RAd-IGF-1 treatment improves spatial memory (Pardo et al., 2016) and motor performance (Nishida et al., 2011) of aged rats.

In the present work, we expanded our knowledge about how IGF-1 gene therapy affects other brain functions in aged rats. In agreement with previous work (Nishida et al., 2011), we observed that IGF-1 treatment improved the motor performance of aged rats in a grip strength test, which was not accompanied by differences in locomotion. Regarding innate behaviour to bury objects, we did not observe significant differences between control and IGF-1 treated groups. This is in accordance with the fact that this behaviour is not altered with aging (Konsolaki et al., 2016). Furthermore, the improvement in motor performance was not accompanied by any alternation in the three points of the dopamine system analysed with different molecular techniques.

Considering these results and taking into account that the CPu is a main area involved in the execution of movement, and that in aged rats IGF-1 gene therapy increases the number and reactivity of microglial cells specifically in this area (Falomir-Lockhart et al., 2019), we decided to partially characterize microglia phenotype. Aging induces microglia to adopt a dystrophic morphology displaying a pro-inflammatory phenotype (Norden and Godbout, 2013), which could damage the surrounding tissue, leading to functional impairment. In the present work, we observed that, after RAd-IGF-1 treatment, more microglia/macrophages in the CPu presented a positive signal for Arginase 1, enzyme that has been

associated with a neuroprotective phenotype (Yang and Ming, 2014). These results led us to consider that IGF-1 gene therapy could be modifying the pro-inflammatory environment and/or pro-inflammatory microglial/macrophages state, characteristic of aging, thus establishing a favourable scenario and an improvement in motor outcome.

We also analysed how IGF-1 gene therapy could modify the CPu environment by using deep RNA sequencing of CPu from aged rats treated with either RAd-IGF-1 or control vector. We found 97 differentially expressed genes (DEG), all downregulated, in the IGF-1 group compared to control. In addition, we compared our DEG list with a list of genes obtained from a meta-analysis in mammals where 225 were identified to be over-expressed during aging. We observed that IGF-1 gene therapy was capable to downregulate 12 of these genes. Among these genes, there are many related with microglia functions such as classical or non-classical complement activation (C3, C1s, C1r) that leads to neuronal and synaptic loss and altered microglial phagocytic activity; pro-inflammatory response (CD74, CP, PSMB8, PLEK); apoptosis or cognitive decline (GBP2, B2M, PLEK, CXCL16); cytotoxicity (FCGR3A); and immune function (RT1-Bb) (see Table 1 for citations).. Furthermore, we observed that the over-expression of these 12 genes has been associated to different pathologies of the CNS related to neuroinflammation and/or aging. These results support our hypothesis that IGF-1 gene therapy is able to modulate the pro-inflammatory CPu microenvironment, thus counteracting the effects of aging neuroinflammation and improving motor functions among other behaviours.

Our data reinforce the potential of IGF-1 as a therapeutic molecule. Nevertheless, further studies should be carried out in order to clarify the mechanism by which this growth factor is modulating the pro-inflammatory environment and microglia/macrophages activation. A better understanding of the mechanisms that modify these cells´ phenotype could contribute to the comprehension of molecular changes involved in the process of inflammation. In this regard, a transcriptomic analysis of isolated microglial/macrophages cells would give us the required information to determine the inflammatory state of these cells. Moreover, studies regarding microglia's phagocytic activity and synaptic remodelling could help understand a possible relation between these cells and the improvement in motor performance. These approaches remain open for future work.

. Our findings could be helpful to the development of novel therapeutic strategies to ameliorate the deterioration of the aged brain.

Conclusion

In summary, our results demonstrate that ICV-IGF-1 gene therapy is able to modulate microglia phenotype by incrementing Arg1 expression. The therapy also modified inflammatory environment and CPu gene expression measured by RNA seq, leading to an improvement in motor function.

Abbreviations

Arg1
arginase 1
CNS
Central Nervous System
CPu
Caudate-Putamen unit
DA
Dopamine
DEGs
differentially expressed genes

DsRed
Red fluorescent protein from Discosoma sp
Iba1
Ionized calcium-binding adapter molecule 1
IGF-1
Insulin-like Growth Factor-1
ICV
Intracerebroventricular
OF
Open Field
RAd
Recombinant Adenoviral vector
TH
Tyrosine Hydroxylase

Declarations

Funding Information

This study was supported by grants from the Argentine Agency for the Promotion of Science and Technology (grant number #PICT13-1119) and the Argentine Research Council (CONICET) (grant number PIP0618) to MJB, grants from the Universidad Nacional de La Plata (grant number M184 to CH and V270 to EP) and grant from the Deutsche Forschungsgemeinschaft (DFG) (grant number SP 1555/2-1) to BS.

Acknowledgements

We thank Natalia Scelsio, Jana Weiß-Müller and Robin Piecha for technical assistance, to Araceli Bigres for animal management, as well as to Dr. Andrea Pereyra for English revision assistance. We acknowledge IBRO and Boehringer Ingelheim Fonds support on EF-L's short stays in Germany.

Author Contribution

EF-L and MJB designed the experiments. EF-L, FJCD, JP and MFVZ performed the experiments. GS performed the RNAseq. EL performed the analysis of the RNAseq. EF-L, FJCD, MLH, EP, EL, CH and MJB analysed the data. EF-L, MLH, EL, BS, CH and MJB wrote the manuscript. All authors have commented on previous versions of the manuscript. All authors read and approved the final manuscript.

Declarations of interest

The authors declare that they do not have conflict of interest.

Data availability statement

The data that support the findings of this study are available from the corresponding author upon reasonable request.

Ethical approval

All experiments with animals have been approved by our institutional Committee for the Care and Use of Laboratory Animals (Protocol #T09-01-2013).

Consent to participate

Not applicable

Consent for publication

Not applicable

References

1. Acaz-Fonseca, E., Duran, J.C., Carrero, P., Garcia-Segura, L.M., Arevalo, M.A., 2015. Sex differences in glia reactivity after cortical brain injury. Glia 63, 1966–1981. https://doi.org/10.1002/glia.22867
2. Alladi, P.A., Mahadevan, A., Yasha, T.C., Raju, T.R., Shankar, S.K., Muthane, U., 2009. Absence of age-related changes in nigral dopaminergic neurons of Asian Indians: Relevance to lower incidence of Parkinson's disease. Neuroscience 159, 236–245. https://doi.org/10.1016/j.neuroscience.2008.11.051
3. Arima, K., Kinoshita, A., Mishima, H., Kanazawa, N., Kaneko, T., Mizushima, T., Ichinose, K., Nakamura, H., Tsujino, A., Kawakami, A., Matsunaka, M., Kasagi, S., Kawano, S., Kumagai, S., Ohmura, K., Mimori, T., Hirano, M., Ueno, S., Tanaka, Keiko, Tanaka, M., Toyoshima, I., Sugino, H., Yamakawa, A., Tanaka, Keiji, Niikawa, N., Furukawa, F., Murata, S., Eguchi, K., Ida, H., Yoshiura, K.I., 2011. Proteasome assembly defect due to a proteasome subunit beta type 8 (PSMB8) mutation causes the autoinflammatory disorder, Nakajo-Nishimura syndrome. Proc. Natl. Acad. Sci. U. S. A. 108, 14914–14919. https://doi.org/10.1073/pnas.1106015108
4. Bassani, T.B., Vital, M.A.B.F., Rauh, L.K., 2015. Neuroinflammation in the pathophysiology of Parkinson's disease and therapeutic evidence of anti-inflammatory drugs. Arq. Neuropsiquiatr. 73, 616–23. https://doi.org/10.1590/0004-282X20150057
5. Bellini, M.J., Hereñú, C.B., Goya, R.G., Garcia-Segura, L.M., 2011. Insulin-like growth factor-I gene delivery to astrocytes reduces their inflammatory response to lipopolysaccharide. J. Neuroinflammation 8, 21. https://doi.org/10.1186/1742-2094-8-21
6. Breese, C.R., D'Costa, A., Rollins, Y.D., Adams, C., Booze, R.M., Sonntag, W.E., Leonard, S., 1996. Expression of insulin-like growth factor-1 (IGF-1) and IGF-binding protein 2 (IGF-BP2) in the hippocampus following cytotoxic lesion of the dentate gyrus. J. Comp. Neurol. 369, 388–404. https://doi.org/10.1002/(SICI)1096-9861(19960603)369:3<388::AID-CNE5>3.0.CO;2-1
7. Carlsson, A., Winblad, B., 1976. Influence of age and time interval between death and autopsy on dopamine and 3-methoxytyramine levels in human basal ganglia. J. Neural Transm. 38, 271–6. https://doi.org/10.1007/bf01249444
8. Chang, H., 2020. PSMB8 inhibition decreases tumor angiogenesis in glioblastoma through vascular endothelial growth factor A reduction 4142–4153. https://doi.org/10.1111/cas.14625
9. de Brouwer, G., Fick, A., Harvey, B.H., Wolmarans, D.W., 2019. A critical inquiry into marble-burying as a preclinical screening paradigm of relevance for anxiety and obsessive–compulsive disorder: Mapping the way forward. Cogn. Affect. Behav. Neurosci. https://doi.org/10.3758/s13415-018-00653-4
10. de Magalhães, J.P., Curado, J., Church, G.M., 2009. Meta-analysis of age-related gene expression profiles identifies common signatures of aging. Bioinformatics 25, 875–881. https://doi.org/10.1093/bioinformatics/btp073
11. Deacon, R.M.J., 2006. Digging and marble burying in mice: Simple methods for in vivo identification of biological impacts. Nat. Protoc. 1, 122–124. https://doi.org/10.1038/nprot.2006.20
12. Deak, F., Sonntag, W.E., 2012. Aging, synaptic dysfunction, and insulin-like growth factor (IGF)-1. Journals Gerontol. - Ser. A Biol. Sci. Med. Sci. 67 A, 611–625. https://doi.org/10.1093/gerona/gls118

13. Di Benedetto, S., Müller, L., Wenger, E., Düzel, S., Pawelec, G., 2017. Contribution of neuroinflammation and immunity to brain aging and the mitigating effects of physical and cognitive interventions. Neurosci. Biobehav. Rev. https://doi.org/10.1016/j.neubiorev.2017.01.044
14. Di Castro, M.A., Trettel, F., Milior, G., Maggi, L., Ragozzino, D., Limatola, C., 2016. The chemokine CXCL16 modulates neurotransmitter release in hippocampal CA1 area. Sci. Rep. 6. https://doi.org/10.1038/srep34633
15. Ding, Y., Kantarci, A., Badwey, J.A., Hasturk, H., Malabanan, A., Van Dyke, T.E., 2007. Phosphorylation of Pleckstrin Increases Proinflammatory Cytokine Secretion by Mononuclear Phagocytes in Diabetes Mellitus. J. Immunol. 179, 647–654. https://doi.org/10.4049/jimmunol.179.1.647
16. Elward, K., Gasque, P., 2003. "Eat me" and "don't eat me" signals govern the innate immune response and tissue repair in the CNS: Emphasis on the critical role of the complement system, in: Molecular Immunology. Elsevier Ltd, pp. 85–94. https://doi.org/10.1016/S0161-5890(03)00109-3
17. Falomir-Lockhart, E., Dolcetti, F.J.C., García-Segura, L.M., Hereñú, C.B., Bellini, M.J., 2019. IGF1 Gene Therapy Modifies Microglia in the Striatum of Senile Rats. Front. Aging Neurosci. 11, 1–6. https://doi.org/10.3389/fnagi.2019.00048
18. Fernandez, A.M., de la Vega, A.G., Torres-Aleman, I., 1998. Insulin-like growth factor I restores motor coordination in a rat model of cerebellar ataxia. Proc. Natl. Acad. Sci. U. S. A. 95, 1253–8. https://doi.org/10.1073/pnas.95.3.1253
19. Fillman, S.G., Cloonan, N., Miller, L.C., Weickert, C.S., 2013. Markers of inflammation in the prefrontal cortex of individuals with schizophrenia. Mol. Psychiatry. https://doi.org/10.1038/mp.2012.199
20. Genis, L., Dávila, D., Fernandez, S., Pozo-Rodrigálvarez, A., Martínez-Murillo, R., Torres-Aleman, I., 2014. Astrocytes require insulin-like growth factor I to protect neurons against oxidative injury. F1000Research 3, 28. https://doi.org/10.12688/f1000research.3-28.v2
21. Guan, J., Bennet, L., George, S., Waldvogel, H.J., Faull, R.L.M., Gluckman, P.D., Keunen, H., Gunn, A.J., 1999. Selective neuroprotective effects with insulin-like growth factor-1 in phenotypic striatal neurons following ischemic brain injury in fetal sheep. Neuroscience 95, 831–839. https://doi.org/10.1016/S0306-4522(99)00456-X
22. Guo, J., Cai, Y., Ye, X., Ma, N., Wang, Y., Yu, B., Wan, J., 2019. MiR-409-5p as a Regulator of Neurite Growth Is Down Regulated in APP/PS1 Murine Model of Alzheimer's Disease. Front. Neurosci. 13, 1264. https://doi.org/10.3389/fnins.2019.01264
23. Habib, A., Sawmiller, D., Hou, H., Kanithi, M., Tian, J., Zeng, J., Zi, D., He, Z.X., Sanberg, P.R., Tan, J., 2018. Human Cord Blood Serum-Derived APP α-Secretase Cleavage Activity is Mediated by C1 Complement. Cell Transplant. 27, 666–676. https://doi.org/10.1177/0963689718775941
24. Harry GJ, 2013. Microglia During Development and Aging. Pharmacol. Ther. 139, 313–326. https://doi.org/10.1016/j.pharmthera.2013.04.013.Microglia
25. Hereñú, C.B., Cristina, C., Rimoldi, O.J., Becú-Villalobos, D., Cambiaggi, V., Portiansky, E.L., Goya, R.G., 2007. Restorative effect of insulin-like growth factor-I gene therapy in the hypothalamus of senile rats with dopaminergic dysfunction. Gene Ther. 14, 237–245. https://doi.org/10.1038/sj.gt.3302870
26. Hereñú, C.B., Sonntag, W.E., Morel, G.R., Portiansky, E.L., Goya, R.G., 2009. The ependymal route for insulin-like growth factor-1 gene therapy in the brain. Neuroscience 163, 442–447. https://doi.org/10.1016/j.neuroscience.2009.06.024
27. Herrera, M.L., Basmadjian, O.M., Falomir-Lockhart, E., Dolcetti, F.J.C., Hereñú, C.B., Bellini, M.J., 2020. Sex frailty differences in ageing mice: Neuropathologies and therapeutic projections. Eur. J. Neurosci. 52, 2827–2837. https://doi.org/10.1111/ejn.14703
28. Hong, S., Beja-Glasser, V.F., Nfonoyim, B.M., Frouin, A., Li, S., Ramakrishnan, S., Merry, K.M., Shi, Q., Rosenthal, A., Barres, B.A., Lemere, C.A., Selkoe, D.J., Stevens, B., 2016. Complement and microglia mediate early synapse loss in

Alzheimer mouse models. Science (80-.). 352, 712–716. https://doi.org/10.1126/science.aad8373

29. Imai, K., Nonoyama, S., Miki, H., Morio, T., Fukami, K., Zhu, Q., Aruffo, A., Ochs, H.D., Yata, J.I., Takenawa, T., 1999. The pleckstrin homology domain of the Wiskott-Aldrich syndrome protein is involved in the organization of actin cytoskeleton. Clin. Immunol. 92, 128–137. https://doi.org/10.1006/clim.1999.4746
30. Johns Hopkins University, A.C. and U.C., n.d. Normative values for rats [WWW Document].
31. JOSEPH, J.A., ROTH, G.S., 1988. Upregulation of Striatal Dopamine Receptors and Improvement of Motor Performance in Senescence. Ann. N. Y. Acad. Sci. 515, 355–362. https://doi.org/10.1111/j.1749-6632.1988.tb33008.x
32. Kim, D., Paggi, J.M., Park, C., Bennett, C., Salzberg, S.L., 2019. Graph-based genome alignment and genotyping with HISAT2 and HISAT-genotype. Nat. Biotechnol. 37, 907–915. https://doi.org/10.1038/s41587-019-0201-4
33. Konsolaki, E., Tsakanikas, P., Polissidis, A. V., Stamatakis, A., Skaliora, I., 2016. Early Signs of Pathological Cognitive Aging in Mice Lacking High-Affinity Nicotinic Receptors. Front. Aging Neurosci. 8, 91. https://doi.org/10.3389/fnagi.2016.00091
34. Labandeira-Garcia, J.L., Costa-Besada, M.A., Labandeira, C.M., Villar-Cheda, B., Rodríguez-Perez, A.I., 2017. Insulin-like growth factor-1 and neuroinflammation. Front. Aging Neurosci. https://doi.org/10.3389/fnagi.2017.00365
35. Lazzaro, M., Bettegazzi, B., Barbariga, M., Codazzi, F., Zacchetti, D., Alessio, M., 2014. Ceruloplasmin potentiates nitric oxide synthase activity and cytokine secretion in activated microglia. J. Neuroinflammation 11, 1–11. https://doi.org/10.1186/s12974-014-0164-9
36. Liao, Y., Smyth, G.K., Shi, W., 2019. The R package Rsubread is easier, faster, cheaper and better for alignment and quantification of RNA sequencing reads. Nucleic Acids Res. 47. https://doi.org/10.1093/nar/gkz114
37. Loeffler, D.A., DeMaggio, A.J., Juneau, P.L., Brickman, C.M., Mashour, G.A., Finkelman, J.H., Pomara, N., LeWitt, P.A., 1994. Ceruloplasmin is increased in cerebrospinal fluid in Alzheimer's disease but not Parkinson's disease. Alzheimer Dis. Assoc. Disord. 8, 190–197. https://doi.org/10.1097/00002093-199408030-00005
38. López-Otín, C., Blasco, M.A., Partridge, L., Serrano, M., Kroemer, G., 2013. The hallmarks of aging. Cell 153, 1194–217. https://doi.org/10.1016/j.cell.2013.05.039
39. Love, M.I., Huber, W., Anders, S., 2014. Moderated estimation of fold change and dispersion for RNA-seq data with DESeq2. Genome Biol. 15, 550. https://doi.org/10.1186/s13059-014-0550-8
40. Luchena, C., Zuazo-Ibarra, J., Alberdi, E., Matute, C., Capetillo-Zarate, E., 2018. Contribution of neurons and glial cells to complement-mediated synapse removal during development, aging and in Alzheimer's disease. Mediators Inflamm. 2018. https://doi.org/10.1155/2018/2530414
41. Miao, Q., Ge, M., Huang, L., 2017. Up-regulation of GBP2 is Associated with Neuronal Apoptosis in Rat Brain Cortex Following Traumatic Brain Injury. Neurochem. Res. 42, 1515–1523. https://doi.org/10.1007/s11064-017-2208-x
42. Mishra, A., Brinton, R.D., 2018. Inflammation: Bridging age, menopause and APOEϵ4 genotype to Alzheimer's disease. Front. Aging Neurosci. https://doi.org/10.3389/fnagi.2018.00312
43. Mlecnik, B., Galon, J., Bindea, G., 2018. Comprehensive functional analysis of large lists of genes and proteins. J. Proteomics 171, 2–10. https://doi.org/10.1016/j.jprot.2017.03.016
44. Morel, G.R., León, M.L., Uriarte, M., Reggiani, P.C., Goya, R.G., 2017. Therapeutic potential of IGF-I on hippocampal neurogenesis and function during aging. Neurogenesis 4, e1259709. https://doi.org/10.1080/23262133.2016.1259709
45. Morgan, D.G., Finch, C.E., 1988. Dopaminergic changes in the basal ganglia. A generalized phenomenon of aging in mammals. Ann. N. Y. Acad. Sci. 515, 145–60. https://doi.org/10.1111/j.1749-6632.1988.tb32978.x
46. Nishida, F., Morel, G.R., Hereñú, C.B., Schwerdt, J.I., Goya, R.G., Portiansky, E.L., 2011. Restorative effect of intracerebroventricular insulin-like growth factor-I gene therapy on motor performance in aging rats. Neuroscience

177, 195–206. https://doi.org/10.1016/j.neuroscience.2011.01.013

47. Nishida, F., Zanuzzi, C.N., Sisti, M.S., Falomir Lockhart, E., Camiña, A.E., Hereñú, C.B., Bellini, M.J., Portiansky, E.L., 2020. Intracisternal IGF-1 gene therapy abrogates kainic acid-induced excitotoxic damage of the rat spinal cord, European Journal of Neuroscience. https://doi.org/10.1111/ejn.14876
48. Norden, D.M., Godbout, J.P., 2013. Review: Microglia of the aged brain: primed to be activated and resistant to regulation. Neuropathol. Appl. Neurobiol. 39, 19–34. https://doi.org/10.1111/j.1365-2990.2012.01306.x
49. Orihuela, R., McPherson, C.A., Harry, G.J., 2016. Microglial M1/M2 polarization and metabolic states. Br. J. Pharmacol. 173, 649–665. https://doi.org/10.1111/bph.13139
50. Pardo, J., Uriarte, M., Cónsole, G.M., Reggiani, P.C., Outeiro, T.F., Morel, G.R., Goya, R.G., 2016. Insulin-like growth factor-I gene therapy increases hippocampal neurogenesis, astrocyte branching and improves spatial memory in female aging rats. Eur. J. Neurosci. 44, 2120–2128. https://doi.org/10.1111/ejn.13278
51. Parkinson, G.M., Dayas, C. V., Smith, D.W., 2015. Age-related gene expression changes in substantia nigra dopamine neurons of the rat. Mech. Ageing Dev. 149, 41–49. https://doi.org/10.1016/j.mad.2015.06.002
52. Paxinos, G., Watson, C., 2007. The Rat Brain in Stereotaxic Coordinates, 6th Editio. ed. Elsevier.
53. Piriz, J., Muller, A., Trejo, J.L., Torres-Aleman, I., 2011. IGF-I and the aging mammalian brain. Exp. Gerontol. 46, 96–99. https://doi.org/10.1016/j.exger.2010.08.022
54. Poling, A., Cleary, J., Monaghan, M., 1981. BURYING BY RATS IN RESPONSE TO AVERSIVE AND NONAVERSIVE STIMULI. J. Exp. Anal. Behav. 35, 31–44. https://doi.org/10.1901/jeab.1981.35-31
55. Sekar, S., McDonald, J., Cuyugan, L., Aldrich, J., Kurdoglu, A., Adkins, J., Serrano, G., Beach, T.G., Craig, D.W., Valla, J., Reiman, E.M., Liang, W.S., 2015. Alzheimer's disease is associated with altered expression of genes involved in immune response and mitochondrial processes in astrocytes. Neurobiol. Aging 36, 583–591. https://doi.org/10.1016/j.neurobiolaging.2014.09.027
56. Shen, G., Mao, Y., Su, Z., Du, J., Yu, Y., Xu, F., 2020. Biomedicine & Pharmacotherapy PSMB8-AS1 activated by ELK1 promotes cell proliferation in glioma via regulating miR-574-5p / RAB10. Biomed. Pharmacother. 122, 109658. https://doi.org/10.1016/j.biopha.2019.109658
57. Shen, Y., Lue, L.F., Yang, L.B., Roher, A., Kuo, Y.M., Strohmeyer, R., Goux, W.J., Lee, V., Johnson, G.V.W., Webster, S.D., Cooper, N.R., Bradt, B., Rogers, J., 2001. Complement activation by neurofibrillary tangles in Alzheimer's disease. Neurosci. Lett. 305, 165–168. https://doi.org/10.1016/S0304-3940(01)01842-0
58. Shi, Q., Chowdhury, S., Ma, R., Le, K.X., Hong, S., Caldarone, B.J., Stevens, B., Lemere, C.A., 2017. Complement C3 deficiency protects against neurodegeneration in aged plaque-rich APP/PS1 mice. Sci. Transl. Med. 9. https://doi.org/10.1126/scitranslmed.aaf6295
59. Shi, Q., Colodner, K.J., Matousek, S.B., Merry, K., Hong, S., Kenison, J.E., Frost, J.L., Le, K.X., Li, S., Dodart, J.C., Caldarone, B.J., Stevens, B., Lemere, C.A., 2015. Complement C3-deficient mice fail to display age-related hippocampal decline. J. Neurosci. 35, 13029–13042. https://doi.org/10.1523/JNEUROSCI.1698-15.2015
60. Shoham, S., Linial, M., Weinstock, M., 2019. Age-Induced Spatial Memory Deficits in Rats Are Correlated with Specific Brain Region Alterations in Microglial Morphology and Gene Expression. J. Neuroimmune Pharmacol. 14, 251:262. https://doi.org/10.1007/s11481-018-9817-2
61. Stark, A.K., Pakkenberg, B., 2004. Histological changes of the dopaminergic nigrostriatal system in aging. Cell Tissue Res. https://doi.org/10.1007/s00441-004-0972-9
62. Suh, H.-S., Zhao, M.-L., Derico, L., Choi, N., Lee, S.C., 2013. Insulin-like growth factor 1 and 2 (IGF1, IGF2) expression in human microglia: differential regulation by inflammatory mediators. J. Neuroinflammation 10, 805. https://doi.org/10.1186/1742-2094-10-37

63. Surugiu, R., Catalin, B., Dumbrava, D., Gresita, A., Olaru, D.G., Hermann, D.M., Popa-Wagner, A., 2019. Intracortical Administration of the Complement C3 Receptor Antagonist Trifluoroacetate Modulates Microglia Reaction after Brain Injury. Neural Plast. 2019. https://doi.org/10.1155/2019/1071036
64. Swanson, M.E.V., Scotter, E.L., Smyth, L.C.D., Murray, H.C., Ryan, B., Turner, C., Faull, R.L.M., Dragunow, M., Curtis, M.A., 2020. Identification of a dysfunctional microglial population in human Alzheimer's disease cortex using novel single-cell histology image analysis. Acta Neuropathol. Commun. 8, 1–16. https://doi.org/10.1186/s40478-020-01047-9
65. Thomas, A., Burant, A., Bui, N., Graham, D., Yuva-Paylor, L.A., Paylor, R., 2009. Marble burying reflects a repetitive and perseverative behavior more than novelty-induced anxiety. Psychopharmacology (Berl). 204, 361–373. https://doi.org/10.1007/s00213-009-1466-y
66. Torres Aleman, I., 2012. Insulin-Like Growth Factor-1 and Central Neurodegenerative Diseases. Endocrinol. Metab. Clin. North Am. 41, 395–408. https://doi.org/10.1016/j.ecl.2012.04.016
67. Umegaki, H., Roth, G.S., Ingram, D.K., 2008. Aging of the striatum: Mechanisms and interventions. Age (Omaha). 30, 251–261. https://doi.org/10.1007/s11357-008-9066-z
68. Von Bohlen Und Halbach, O., 2013. Analysis of morphological changes as a key method in studying psychiatric animal models. Cell Tissue Res. https://doi.org/10.1007/s00441-012-1547-9
69. Wood, S.H., Craig, T., Li, Y., Merry, B., De Magalhães, J.P., 2013. Whole transcriptome sequencing of the aging rat brain reveals dynamic RNA changes in the dark matter of the genome. Age (Omaha). 35, 763–776. https://doi.org/10.1007/s11357-012-9410-1
70. Yang, Z., Ming, X.-F., 2014. Functions of Arginase Isoforms in Macrophage Inflammatory Responses: Impact on Cardiovascular Diseases and Metabolic Disorders. Front. Immunol. 5, 533. https://doi.org/10.3389/fimmu.2014.00533
71. Zhao, J., Xu, C., Cao, H., Zhang, L., Wang, X., Chen, S., 2019. Identification of target genes in neuroinflammation and neurodegeneration after traumatic brain injury in rats. PeerJ 2019, e8324. https://doi.org/10.7717/peerj.8324
72. Zhong, Q., Zou, Y., Liu, H., Chen, T., Zheng, F., Huang, Y., Chen, C., 2020. Toll-like receptor 4 deficiency ameliorates β 2-microglobulin induced age-related cognition decline due to neuroinflammation in mice 1–15.

Figures

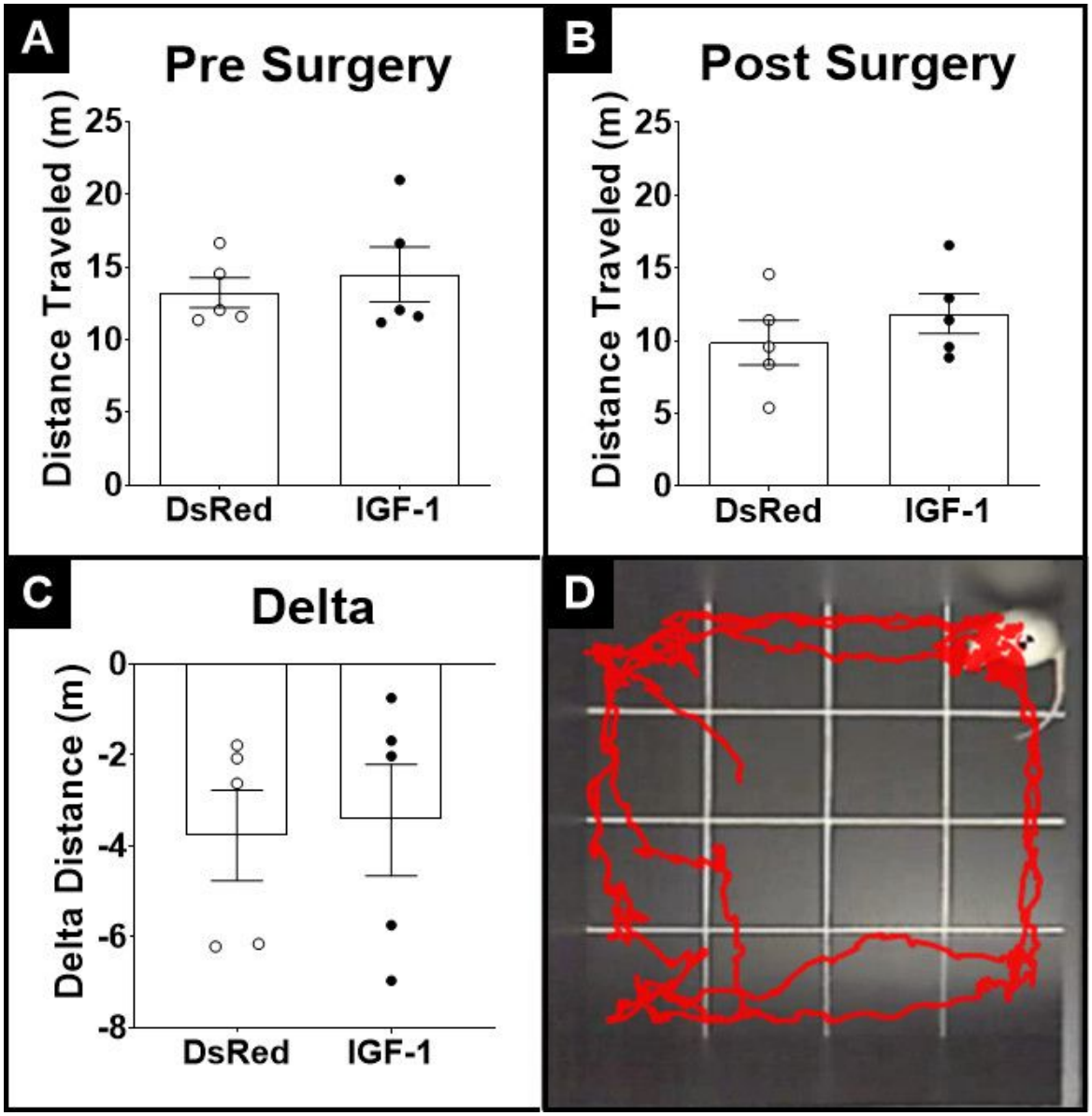

Figure 1

Effect of IGF-1 gene therapy on the locomotion of aged rats. Panels show the distance travelled before (A) and after (B) RAd-IGF-1 treatment. Panel C shows the difference in the distance travelled between time points for each group calculated as “Δ Performance = (Distance post-treatment – Distance pre-treatment)”. Panel (D) shows a representative tracing. Data are given as means ± SEM (N = 5/group). *Significant differences ($p < 0.05$).

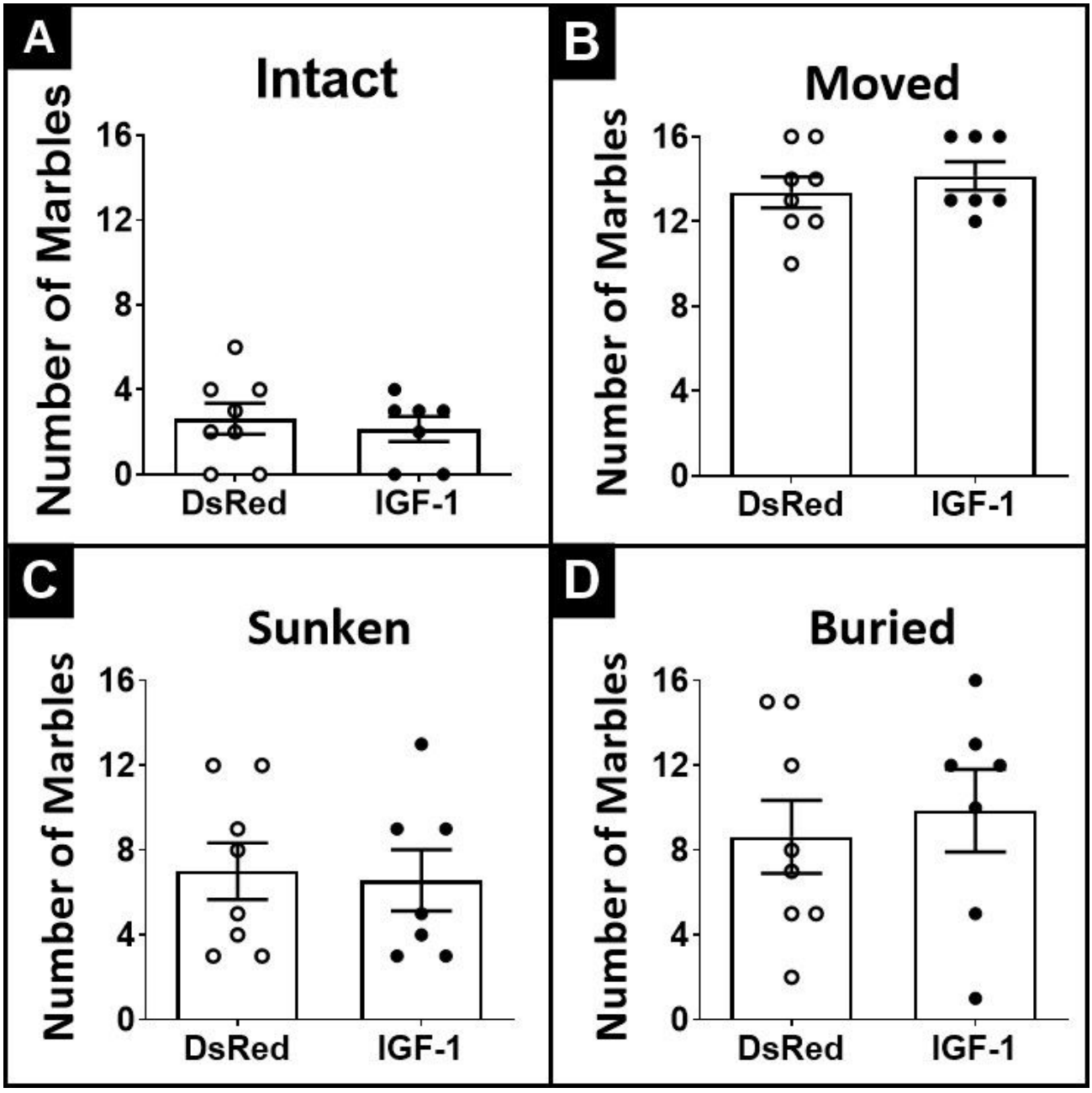

Figure 2

Effect of IGF-1 gene therapy on the innate burying behaviour of aged rats. Panels A-D show the number of intact, moved, sunken or buried marbles. (A) Intact marbles: marbles without being moved or sunken. (B) Moved marbles: marbles moved from their original position with or without being buried. (C) Sunken marbles: marbles buried 2/3 of their totality. (D) Buried marbles: marbles buried in their totality. Data are given as means ± SEM (N = 8/group).

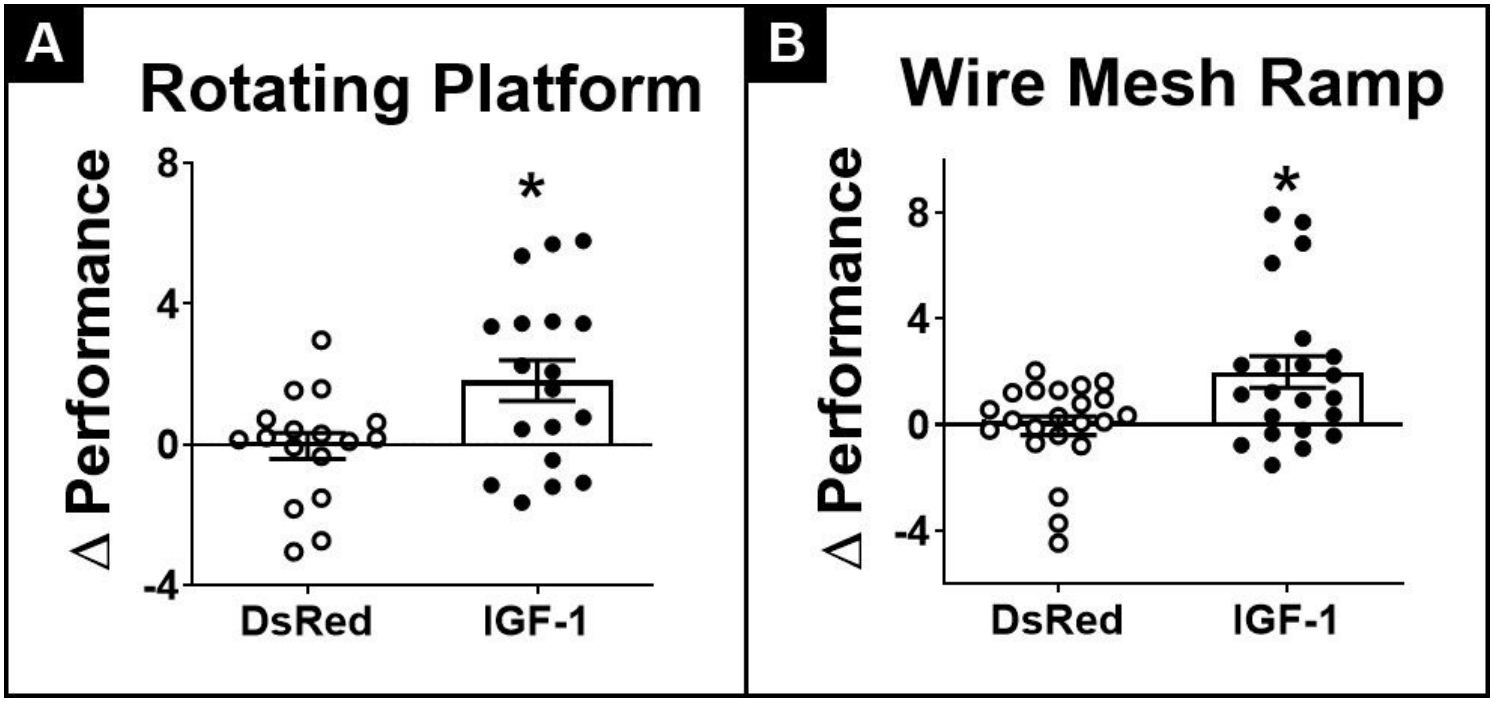

Figure 3

Effect of IGF-1 gene therapy on Motor Performance. Panels show the motor performance of aged rats on a Rotating Platform (A) or on a Wire Mesh Ramp set at 70° (B). Δ Performance (Time post-treatment – Time pre-treatment). Data are given as means ± SEM (N = 21-24/group). * Significant differences ($p < 0.01$).

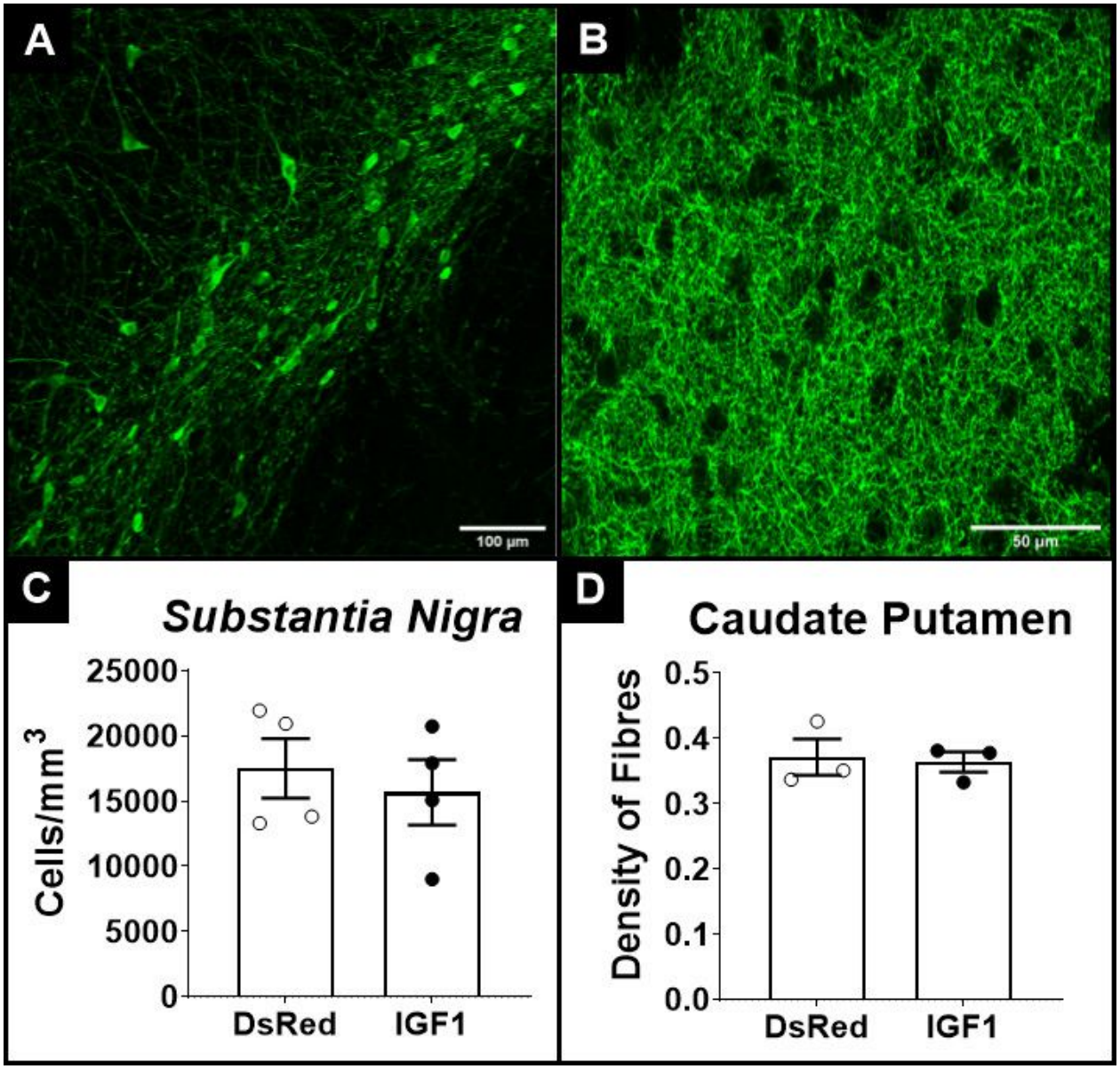

Figure 4

Effect of IGF-1 gene therapy on dopaminergic neurons. Panels show representative TH staining of the Substantia Nigra (A) and the CPu (B) at a magnification of 20X and 60X respectively. Quantification of DA neurons in the Substantia Nigra (C) and the density of fibres in the CPu (D) was assessed in both experimental groups. Data are given as means ± SEM ($N \geq 3$/group).

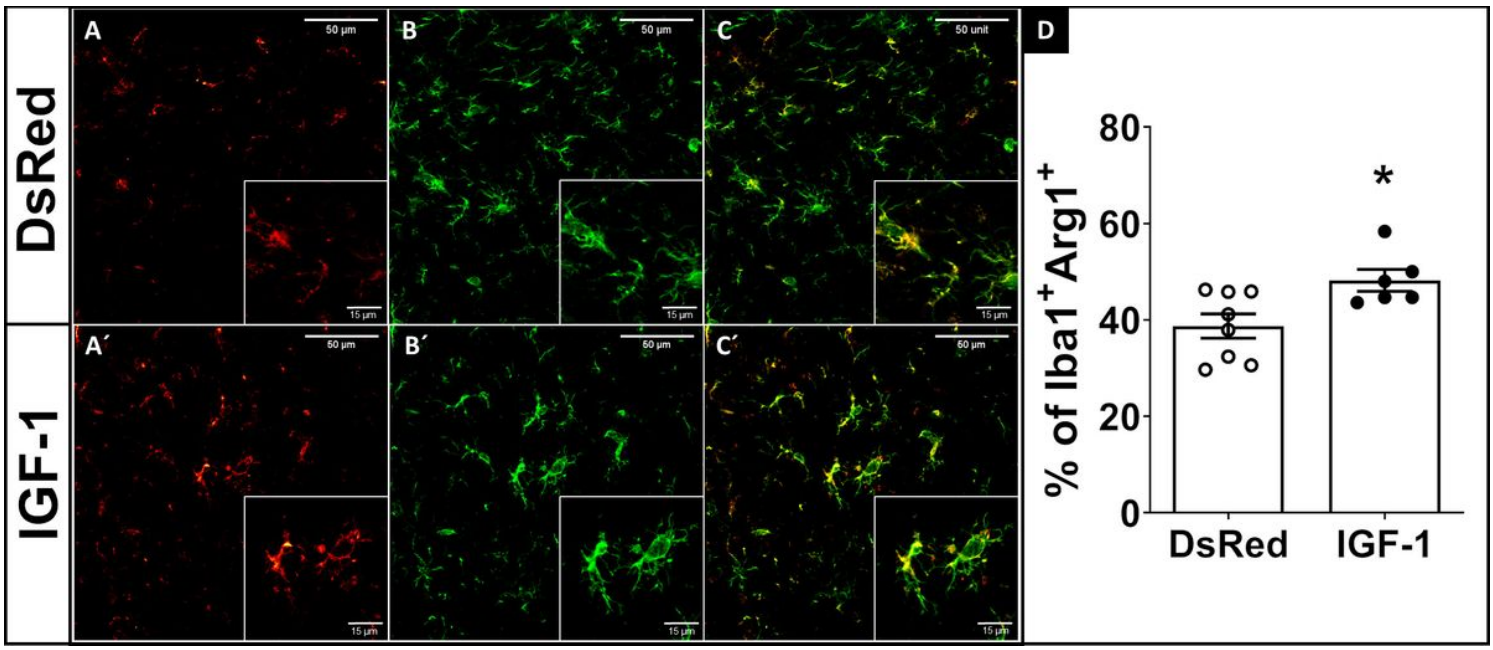

Figure 5

Effect of IGF-1 gene therapy on microglial inflammatory phenotype in the Cpu. Panels show Arginase-positive cells (A, A'), Iba1-positive cells (B, B') and the merge of both fluorescent channels (C, C') in the CPu of DsRed (A, B, C) and IGF-1 (A', B', C') rats, at a magnification of 20X. Panel D shows the percentage of double immunostained (Iba1+Arg1+) on total microglia in CPu. Data are given as means ± SEM (N > 6/group). * Significant differences ($p < 0.05$).

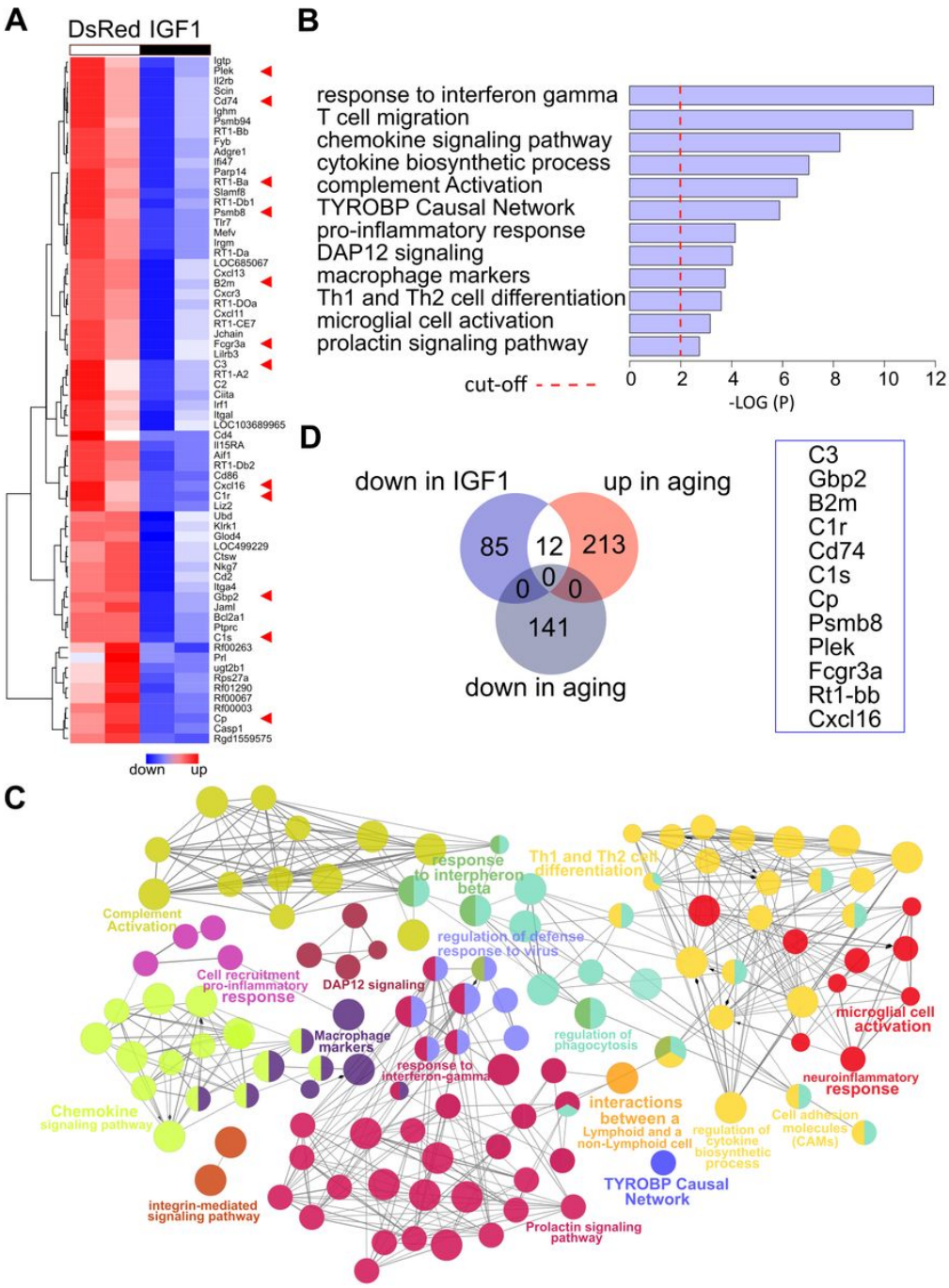

Figure 6

Transcriptional effects of IGF-1 therapy in rat CPu. (A) Heat map representation of the top 70 differentially expressed genes (DEGs) out of 98, obtained from the comparison between CPu samples from IGF-1 and DsRed rats (B). Functional enrichment analysis based on the 98 DEGs obtained from the RNAseq comparison. The red dashed line indicates the cut-off line where the p value is = 0.01 (C) Functional enrichment network of the biological terms associated to the list of DEGs. A total of 14 color-coding clusters can be observed ($p<0.001$), for which one or more representative biological terms are indicated (the detailed list of groups and ontological terms can be found in Table S2). (D) Venn diagram showing common genes between IGF-1-DEGs (down in IGF-1) and the meta-analysis dataset (up in aging and down in aging. The 12 common genes are shown in the blue box and are pointed out with red arrowheads along the heat map in (A).

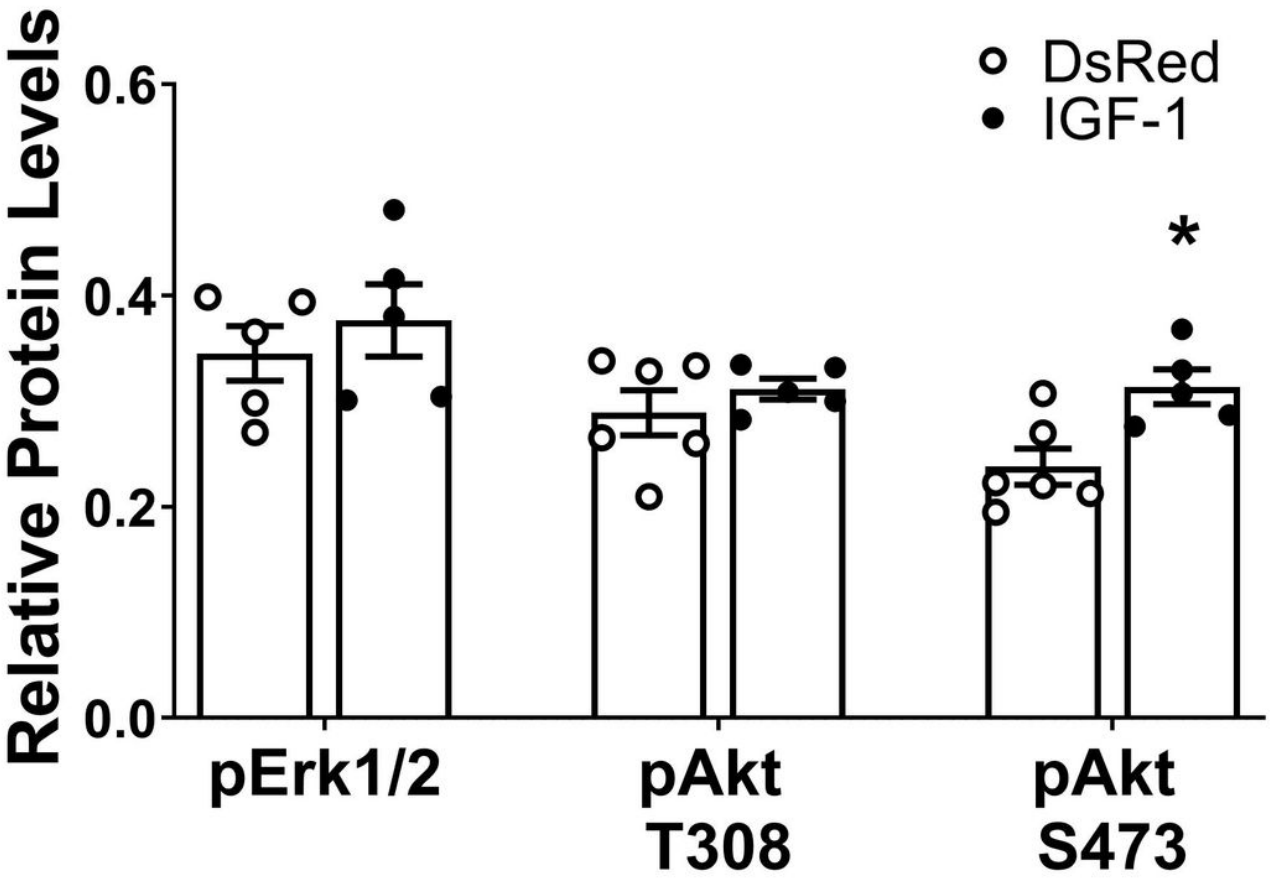

Figure 7

Effect of IGF-1 gene therapy on IGF-1 pathway activation. This graph shows the relative levels of pErk, pAkt Thr308 and Akt Ser473, normalized to the endogenous positive control of the PathScan® Intracellular Signaling Array Kit, in the CPu of rats treated with either RAd-DsRed o RAd-IGF-1. Data are given as means ± SEM (N ≥ 4/group). * Significant differences ($p < 0.05$).

Supplementary Files

This is a list of supplementary files associated with this preprint. Click to download.

- FigureS1.jpg
- FigureS2.jpg
- FigureS3.jpg
- SupplementarymaterialTableS1.xlsx
- SupplementarymaterialTableS2.xlsx